Geochemical Perspectives Letters

Molybdenum isotope constraints on the temporal development of sulfidic conditions during Mediterranean sapropel intervals

T. Sweere[1,2*], R. Hennekam[1,2], D. Vance[2], G.-J. Reichart[1,3]

OPEN ACCESS

doi: 10.7185/geochemlet.2108

Abstract

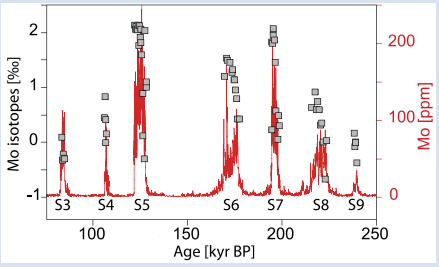

Mediterranean sapropels represent some of the largest scale deoxygenation events in recent Earth history. Here, we use high resolution Mo isotope data for seven such events (sapropels S3 to S9) to semi-quantitatively constrain past H_2S concentrations using a new interpretive framework. Bottom water H_2S was present for all studied sapropels, but the extent of redox changes varied considerably between them, the ultimate driver likely being variations in monsoon strength. Near-quantitative removal of Mo ($\delta^{98}Mo > 2$ ‰) during deposition of sapropels S5 and S7 suggests predominantly highly sulfidic conditions with long deep water residence times, comparable to the modern Black Sea, whereas considerably lower $\delta^{98}Mo$ values for sapropels S3, S4, S8, and S9 (−0.4 to +0.9 ‰) imply mildly euxinic conditions only ($0 < H_2S < 11$ µmol/L). The high resolution data reveal consistent temporal patterns that track the development of basin restriction and euxinia over several kyr. These observations illustrate how Mo isotopes can provide quantitative constraints on basin wide redox changes on relatively short time scales.

Received 13 October 2020 | Accepted 22 January 2021 | Published 18 February 2021

Introduction

Reconstructions of past deoxygenation events from the sedimentary record are crucial in improving projections of future deoxygenation and associated perturbations to biogeochemical cycles. Organic-rich sapropel layers in the Mediterranean reflect some of the largest scale basin deoxygenation events in recent Earth history. The setting allows the study of repeated intervals of basin deoxygenation of various intensities, at high resolution and within a well established stratigraphic framework.

The timing of Mediterranean sapropel deposition is controlled by maxima in Northern hemisphere summer insolation during precession minima, which lead to higher monsoon intensity over the North African continent (*e.g.*, Ziegler *et al.*, 2010; Grant *et al.*, 2016). Greater freshwater input resulted in nutrient-rich conditions, enhanced water column stratification, and a decrease in local deep water formation, which ultimately caused the drawdown of dissolved oxygen at depth and the deposition of sapropels (*e.g.*, Rohling *et al.*, 2015). As the environmental boundary conditions during these events are relatively well established, sapropels present excellent analogues for intermittent anoxic and sulfidic conditions in past ocean basins (*e.g.*, Dahl *et al.*, 2019) as well as targets for modelling efforts aiming to address large scale basin deoxygenation, provided that redox conditions are quantitatively constrained.

Molybdenum (Mo) concentrations of marine sediments are well established as a tracer for local marine redox conditions, while its isotopes have more recently emerged as a valuable proxy to estimate redox conditions on local to global spatial scales (*e.g.*, Scott and Lyons, 2012; Kendall *et al.*, 2017 and references therein). In oxic waters, dissolved Mo is mostly present as the molybdate ion (MoO_4^{2-}), which behaves conservatively. However, in the presence of H_2S, conversion of molybdate to particle-reactive thiomolybdate species ($MoO_{4-x}S_x^{2-}$) results in the enhanced export and burial of Mo (Erickson and Helz, 2000). High sedimentary Mo enrichments can thus be taken to reflect sulfidic water column conditions (*e.g.*, Scott and Lyons, 2012).

The Mo isotope composition of organic-rich sediments is generally lighter than seawater (2.34 ‰; Nakagawa *et al.*, 2012), with reported $\delta^{98}Mo$ values as low as ~ −0.7 ‰ (*e.g.*, Andersen *et al.*, 2020; Brüske *et al.*, 2020). Low $\delta^{98}Mo$ values in mildly euxinic environments can be attributed to isotope fractionation associated with the incomplete conversion of molybdate to thiomolybdate species, with the more sulfidised species becoming progressively isotopically lighter (Tossell, 2005; Kerl *et al.*, 2017). Large isotopic differences between sediments and seawater for such sediments can be modelled by the kinetically controlled preferential scavenging of the more sulfidised thiomolybdate species (Dahl *et al.*, 2010; Matthews *et al.*, 2017). Sedimentary Mo isotope values only approach the original seawater composition in strongly restricted and euxinic basins (*e.g.*, Neubert *et al.*, 2008; Brüske *et al.*, 2020). Mo isotope data have been published previously only for sapropels S1 and S5 and show highly contrasting values. High $\delta^{98}Mo$ (up to ~2.3 ‰) values have been found for S5, reflecting strongly euxinic conditions with long deep water renewal times (Andersen *et al.*, 2018). By contrast,

1. NIOZ Royal Netherlands Institute for Sea Research and Utrecht University, Texel, The Netherlands
2. Institute of Geochemistry and Petrology, Department of Earth Sciences, ETH Zürich, Zürich, Switzerland
3. Department of Earth Sciences, Utrecht University, Utrecht, The Netherlands
* Corresponding author (email: tim.sweere@erdw.ethz.ch)

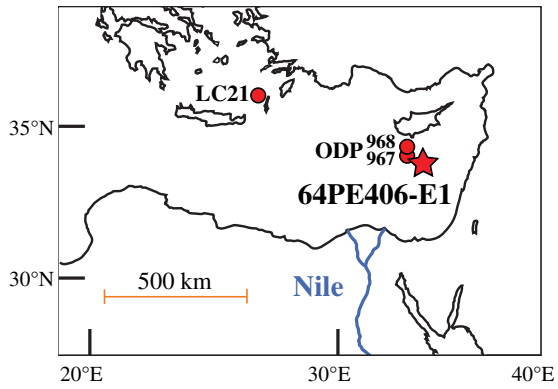

Figure 1 Location of piston core 64PE406-E1 (this study), the LC21, and ODP 968 cores used for the age model, and ODP 967 studied by Andersen *et al.* (2018).

low δ^{98}Mo values (mostly <1 ‰) have been found for sapropel S1, indicating on average lower bottom water H_2S concentrations (Reitz *et al.*, 2007; Azrieli-Tal *et al.*, 2014; Matthews *et al.*, 2017; Andersen *et al.*, 2020).

The Eastern Mediterranean is punctuated by at least 6 further deoxygenation events during the last ~300 kyr, but basin redox conditions have not been quantitatively constrained for these periods. Here, we provide semi-quantitative constraints on bottom water H_2S concentrations for these recent short lived (<10^4 years) deoxygenation events in the Eastern Mediterranean Sea during deposition of sapropels S3 to S9, that reveal a range of different redox conditions (see Supplementary Information for a description of the methodology and results). High resolution Mo concentration (mm scale) and isotope (cm scale) data allow a detailed assessment of the temporal evolution of the dissolved Mo pool on kyr time scales, which is used to reconstruct the development of deep water redox conditions and residence times.

Discussion

Inter-Sapropel Comparisons. Low δ^{98}Mo values and Mo concentrations for sapropels S3, S4, and S9 of core 64PE406-E1 (Fig. 1; Supplementary Information) are similar to those previously published values for sapropel S1, suggesting that these sediments were deposited under mildly euxinic conditions ($[H_2S] < 11$ µM) (Fig. 2; Azrieli-Tall *et al.*, 2014; Matthews *et al.*, 2017; Andersen *et al.*, 2020). Alternative models for low δ^{98}Mo values for these sediments, such as deposition associated with Fe or Mn (oxyhydr)oxides (*e.g.*, Reitz *et al.*, 2007) are not supported by the Mn, Mo, and U concentration data as these data do not show evidence for a strong Fe-Mn particulate shuttle (Supplementary Information; Figs. S-3 to S-5). High δ^{98}Mo values and Mo concentrations for S5 and S7 can mostly be explained by smaller fractionations and more complete removal from seawater in more euxinic conditions. These same intervals are thought to have experienced the highest monsoon intensity over the North African continent in the last 300 kyr, suggesting a direct link between monsoon strength and degree of basin deoxygenation (Fig. 2; Ziegler *et al.*, 2010; Grant *et al.*, 2016).

Interpretative Framework for Mo Concentrations and Isotopes. Combining Black Sea surface sediment data and a mechanistic understanding of Mo isotope systematics derived from kinetic models (Matthews *et al.*, 2017) may facilitate a more detailed interpretation of sedimentary Mo signals. Surface sediment data from different Black Sea water depths highlights systematic patterns that reflect variations in dissolved Mo and H_2S concentrations (Fig. 3a). A generally good agreement between Black Sea sediment data and models based on higher particle affinities for the more sulfidised thiomolybdate species (Matthews *et al.*, 2017) implies that δ^{98}Mo values may be used to constrain past bottom water H_2S concentrations (Fig. 3b). This relationship between sedimentary δ^{98}Mo values and $[H_2S]$ depends on (1) Mo speciation as a function of H_2S, (2) fractionation factors between the different Mo species, (3) the isotopic composition of seawater, and (4) particle affinities of the different thiomolybdate species. Currently, the largest uncertainty in this approach is associated with particle affinities because these are not constrained by direct measurements. Particle affinities for different thiomolybdate species can be described by partition coefficients, *i.e.* $K_i = [MoO_{4-i}S_i^{2-}]_{particulate}/[MoO_{4-i}S_i^{2-}]_{dissolved}$, with i being the number of S atoms (Dahl *et al.*, 2010). Previously, much higher particle affinities for the more sulfidised species have been proposed (K_0, K_1, K_2, K_3, $K_4 = 0$, 0, 1, 25, 100) but these

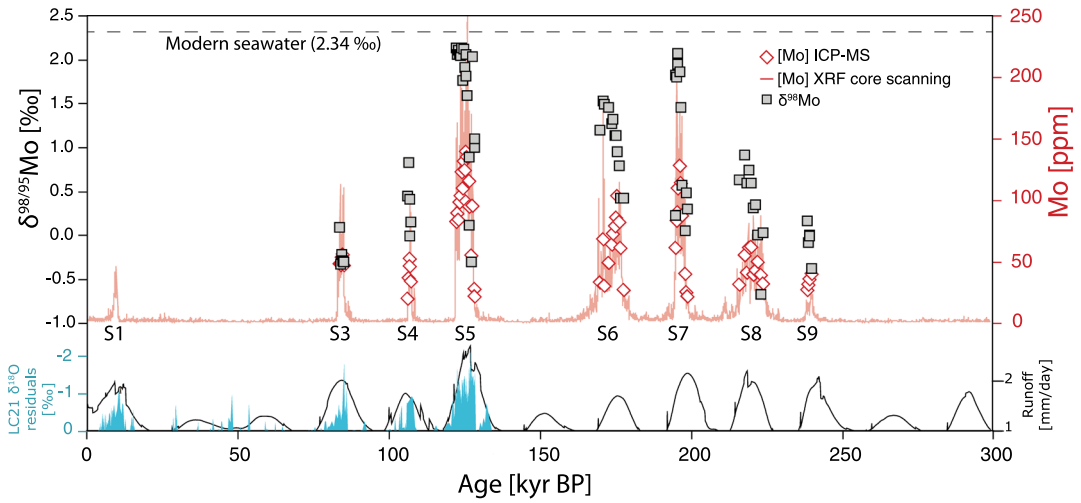

Figure 2 δ^{98}Mo and Mo concentration data for core 64PE406-E1. The bottom panel reflects indicators of monsoon-driven freshwater input. LC21 core 'residuals' (blue) show the $\delta^{18}O_{G.\ ruber}$ values up to 150 ka BP after correction for a seawater effect (Grant *et al.*, 2016). The black line shows the modelled North African run off (CLIMBER-2; Ziegler *et al.*, 2010). XRF core scanning data by Hennekam *et al.* (2020). The uncertainties (2 s.d.) on the Mo isotope data are smaller than the symbol sizes.

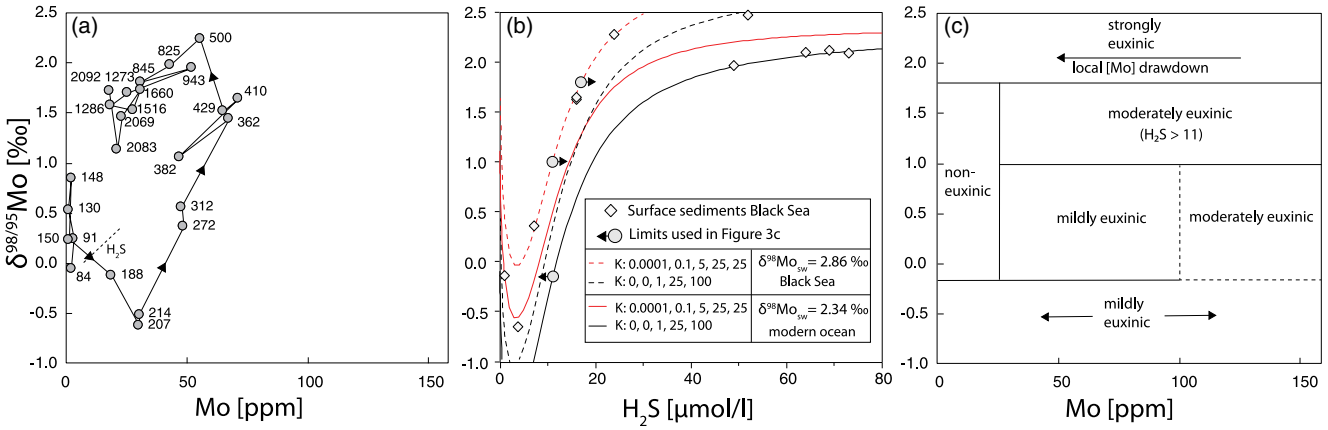

Figure 3 Mo isotope systematics. **(a)** Surface sediment (0–1 cm depth) data from different water depths (as data labels) in the modern Black Sea (Neubert *et al.*, 2008; Brüske *et al.*, 2020). **(b)** Sedimentary δ^{98}Mo values as a function of aqueous H_2S concentrations following calculations by Matthews *et al.* (2017) for different relative particle affinities and seawater δ^{98}Mo. The 2.86 ‰ value is the average of deep Black Sea water compositions (Nägler *et al.*, 2011). $\delta^{98}Mo_{seawater}$ can evolve to higher values in strongly restricted basins, such that sediments formed from an evolved water mass might show higher δ^{98}Mo values. The grey circles represent constraints on [H_2S] from δ^{98}Mo that agree with all four models and are therefore used in Figure 3c to constrain [H_2S] conservatively. Sediment data from Neubert *et al.* (2008). **(c)** Framework for the semi-quantitative reconstruction of [H_2S].

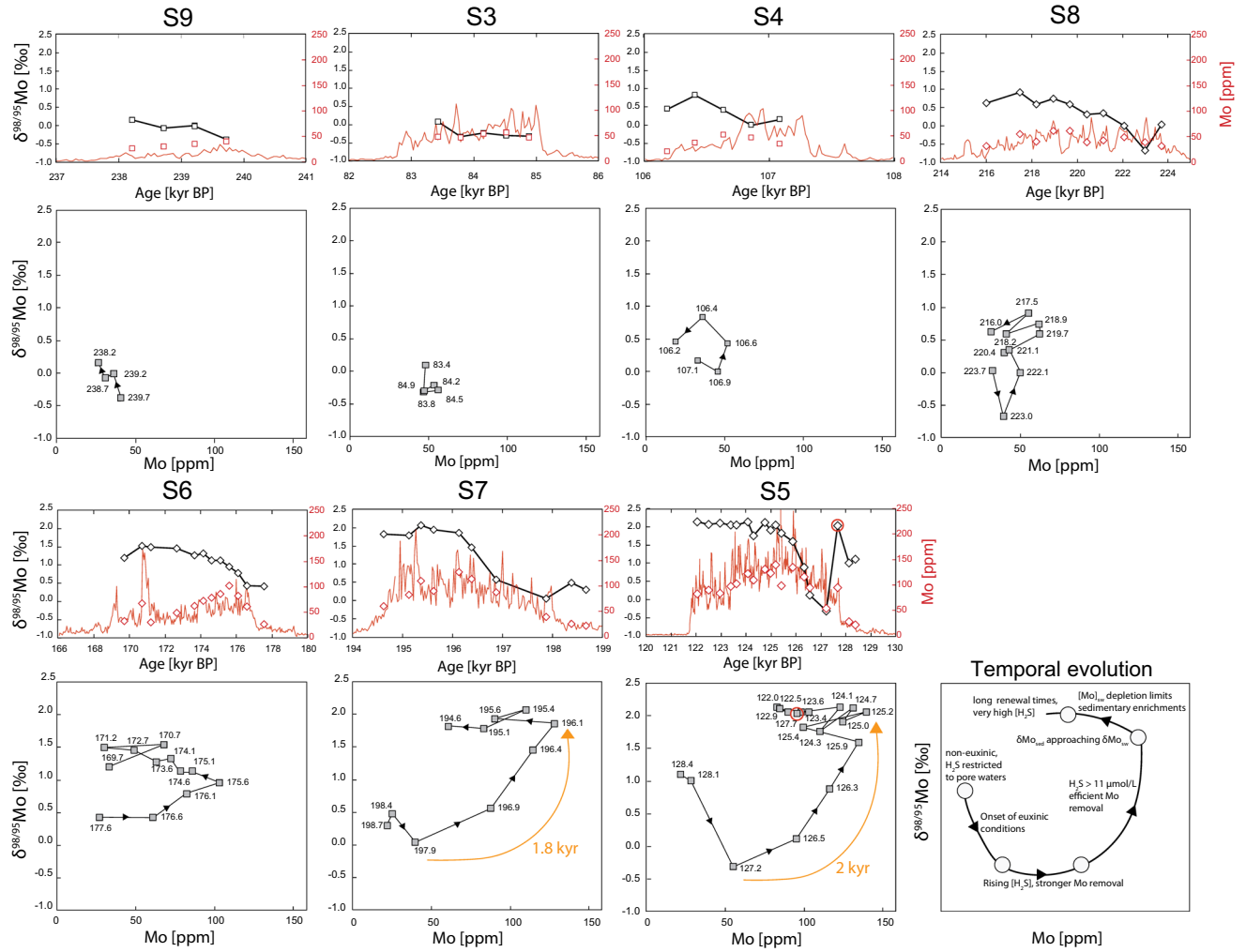

Figure 4 Close up of data presented in Figure 2 for sapropel intervals, including cross plots with age labels. The orange arrows highlight similarities in temporal patterns between S5 and S7. The bottom right plot shows a schematic interpretation of temporal patterns.

values seem to overestimate the fractionation between seawater and sediment for intermediate H_2S concentrations (Fig 3b; Dahl *et al.*, 2010). Tuning the particle affinities to the available Black Sea data (0.0001, 0.1, 5, 25, 25) improves the general fit, although the relative particle affinities remain poorly constrained. Therefore, here we only conservatively estimate [H_2S], by using Mo isotopes to constrain upper or lower limits of past [H_2S] that are valid for a range of different particle affinities (Fig. 3b, c).

Semi-Quantitative Reconstructions of Sapropel Euxinia. We distinguish between four different levels of euxinia, based on the calculations (Matthews *et al.*, 2017) fitted to the Black Sea data (Fig. 3b) with additional constraints from the Mo concentration data (Fig. 3c). Low sedimentary δ^{98}Mo values (< −0.1 ‰) are taken as evidence for mildly euxinic conditions (0 < [H_2S] < 11 μmol/L). Conversely, for high δ^{98}Mo values (>1.8 ‰), the H_2S to δ^{98}Mo relationship flattens such that δ^{98}Mo values can only roughly constrain past H_2S concentrations. These values (δ^{98}Mo > 1.8 ‰) are accordingly taken to reflect dominantly highly sulfidic deep water conditions, with prevailing H_2S concentrations of at least 17 μmol/L, but potentially much higher. δ^{98}Mo values between −0.1 and 1.8 ‰ are less diagnostic by themselves, but can be interpreted considering the Mo concentrations of organic-rich sediments based on the limits for predominantly non-euxinic (<25 ppm), at least temporary euxinic (25–100 ppm), and mostly euxinic (>100 ppm) conditions (Scott and Lyons, 2012). Therefore, reasonably high δ^{98}Mo values (>1 ‰) with concentrations of >25 ppm, and δ^{98}Mo values of at least −0.1 ‰ coupled to high (>100 ppm) Mo concentrations, are both considered to have been deposited in 'moderately euxinic' conditions, where conditions were dominantly sulfidic but with H_2S concentrations low enough to still allow fractionation between sediments and seawater.

Based on this framework, during deposition of sapropels S5 and S7 more sulfidic water column conditions (H_2S > 17 μmol/L) developed. This is in line with the study of Benkovitz *et al.* (2020), who infer euxinic conditions for sapropels S5 and S7 based on Fe isotope and speciation data. By contrast, moderately euxinic bottom water conditions developed during sapropel S6, whereas during sapropels S3, S4, S8, and S9 mildly euxinic conditions were reached (0 < H_2S < 11 μmol/L).

Temporal Patterns in Mo Concentrations and Isotopes. Similar temporal patterns in [Mo] and δ^{98}Mo are observed for different sapropels, particularly for sapropels S5, S6, S7, and S8 (Fig. 4). This general pattern is similar to that defined by Black Sea surface sediments from different water depths (Fig. 3a), which implies that the sapropel S5-S8 data reflect a progressive increase in [H_2S] and evolution of the dissolved Mo pool. The relatively rapid changes in δ^{98}Mo observed here (>2 ‰ in ~2 kyr for S5) show that reconstructions of global redox changes on longer time scales from δ^{98}Mo values in organic-rich sediments come with considerable uncertainty.

Mo Drawdown and Deep Water Renewal Times. The lower Mo concentrations and higher δ^{98}Mo values found for the latter third of sapropels S5 and S7 is in line with progressive drawdown of dissolved Mo under highly sulfidic deep waters with long deep water renewal times, similar to conditions in the modern Black Sea (Nägler *et al.*, 2011). Previous estimates of deep water residence times for sapropel S5 of 1030 +820/−520 years approach that of the modern Black Sea (Andersen *et al.*, 2018). Similarities in δ^{98}Mo and Mo concentrations for sapropel S5 and S7 imply that deep water renewal times for S7 were comparable to that of S5. These results highlight that conditions remained strongly reducing throughout the sapropel, including towards the end of sapropel deposition, despite gradually lower Mo concentrations. The other studied sapropels likely featured lower overall drawdown of dissolved Mo, implying shorter deep water residence times and/or rates of Mo drawdown.

Conclusion

High resolution Mo isotope and concentration data from different Mediterranean sapropels reveal consistent temporal patterns. With the use of models with a kinetic control on the different thiomolybdate species and by comparison to Black Sea data, these patterns can be interpreted to reflect increasingly more sulfidic conditions during the early stages of sapropel formation. The differences between sapropels seem to be driven primarily by changes in monsoon strength over North Africa, and associated run off of freshwater into the Mediterranean Sea. As such, these data highlight an under-appreciated ability of Mo isotope data to quantitatively constrain basin redox changes over several kyr. The highly variable Mo isotope values on relatively short (10^3 years) time scales show that Mo isotopes should be used with great care when reconstructing global ocean redox conditions from black shales.

Acknowledgements

We thank the captain and crew of the R/V *Pelagia* cruise 64PE406, carried out under NESSC programme and financially supported by the Netherlands Ministry of OCW, grant number 024.002.001. We are thankful to B. van der Wagt, P. Laan, M. Klaver, and A. Dickson for analytical support. RH is supported through NWO grant ALW OP.2015.113 awarded to G.-J.R. Constructive comments by Tais Dahl and two anonymous reviewers have helped us to improve our manuscript.

Editor: Sophie Opfergelt

Additional Information

Supplementary Information accompanies this letter at https://www.geochemicalperspectivesletters.org/article2108.

Cite this letter as: Sweere, T., Hennekam, R., Vance, D., Reichart, G.-J. (2021) Molybdenum isotope constraints on the temporal development of sulfidic conditions during Mediterranean sapropel intervals. *Geochem. Persp. Let.* 17, 16–20.

References

Andersen, M.B., Matthews, A., Vance, D., Bar-Matthews, M., Archer, C., de Souza, G. (2018) A 10-fold decline in the deep Eastern Mediterranean thermohaline overturning circulation during the last interglacial period. *Earth and Planetary Science Letters* 503, 58–67.

Andersen, M.B., Matthews, A., Bar-Matthews, M., Vance, D. (2020) Rapid onset of ocean anoxia shown by high U and low Mo isotope compositions of sapropel S1. *Geochemical Perspectives Letters* 15, 10–14.

Azrieli-Tal, I., Matthews, A., Bar-Matthews, M., Almogi-Labin, A., Vance, D., Archer, C., Teutsch, N. (2014) Evidence from molybdenum and iron isotopes and molybdenum–uranium covariation for sulphidic bottom waters during Eastern Mediterranean sapropel S1 formation. *Earth and Planetary Science Letters* 393, 231–242.

Benkovitz, A., Matthews, A., Teutsch, N., Poulton, S.W., Bar-Matthews, M., Almogi-Labin, A. (2020) Tracing water column euxinia in Eastern Mediterranean Sapropels S5 and S7. *Chemical Geology*, 119627.

Brüske, A., Weyer, S., Zhao, M.-Y., Planavsky, N., Wegwerth, A., Neubert, N., Dellwig, O., Lau, K., Lyons, T. (2020) Correlated molybdenum and uranium isotope signatures in modern anoxic sediments: Implications for their use as paleo-redox proxy. *Geochimica et Cosmochimica Acta* 270, 449–474.

Dahl, T.W., Anbar, A.D., Gordon, G.W., Rosing, M.T., Frei, R., Canfield, D.E. (2010) The behavior of molybdenum and its isotopes across the chemocline and in the sediments of sulfidic Lake Cadagno, Switzerland. *Geochimica et Cosmochimica Acta* 74, 144–163.

Dahl, T.W., Siggaard-Andersen, M.L., Schovsbo, N.H., Persson, D.O., Husted, S., Hougård, I.W., Dickson, A.J., Kjær, K., Nielsen, A.T. (2019) Brief oxygenation events in locally anoxic oceans during the Cambrian solves the animal breathing paradox. *Scientific Reports* 9, 1–9.

Erickson, B.E., Helz, G.R. (2000) Molybdenum (VI) speciation in sulfidic waters: stability and lability of thiomolybdates. *Geochimica et Cosmochimica Acta* 64, 1149–1158.

Grant, K., Grimm, R., Mikolajewicz, U., Marino, G., Ziegler, M., Rohling, E. (2016) The timing of Mediterranean sapropel deposition relative to insolation, sea-level and African monsoon changes. *Quaternary Science Reviews* 140, 125–141.

Hennekam, R., van der Bolt, B., van Nes, E.H., de Lange, G.J., Scheffer, M., Reichart, G.-J. (2020) Early-warning signals for marine anoxic events. *Geophysical Research Letters* 47, e2020GL089183.

Kendall, B., Dahl, T., Anbar, A.D. (2017) The stable isotope geochemistry of molybdenum. *Reviews in Mineralogy and Geochemistry* 82, 683–732.

Kerl, C.F., Lohmayer, R., Bura-Nakić, E., Vance, D., Planer-Friedrich, B. (2017) Experimental confirmation of isotope fractionation in thiomolybdates using ion chromatographic separation and detection by multicollector ICPMS. *Analytical Chemistry* 89, 3123–3129.

Matthews, A., Azrieli-Tal, I., Benkovitz, A., Bar-Matthews, M., Vance, D., Poulton, S.W., Teutsch, N., Almogi-Labin, A., Archer, C. (2017) Anoxic development of sapropel S1 in the Nile Fan inferred from redox sensitive proxies, Fe speciation, Fe and Mo isotopes. *Chemical Geology* 475, 24–39.

Nägler, T., Neubert, N., Böttcher, M., Dellwig, O., Schnetger, B. (2011) Molybdenum isotope fractionation in pelagic euxinia: evidence from the modern Black and Baltic Seas. *Chemical Geology* 289, 1–11.

Nakagawa, Y., Takano, S., Firdaus, M.L., Norisuye, K., Hirata, T., Vance, D., Sohrin, Y. (2012) The molybdenum isotopic composition of the modern ocean. *Geochemical Journal* 46, 131–141.

Neubert, N., Nägler, T.F., Böttcher, M.E. (2008) Sulfidity controls molybdenum isotope fractionation into euxinic sediments: Evidence from the modern Black Sea. *Geology* 36, 775–778.

Reitz, A., Wille, M., Nägler, T.F., de Lange, G.J. (2007) Atypical Mo isotope signatures in eastern Mediterranean sediments. *Chemical Geology* 245, 1–8.

Rohling, E., Marino, G., Grant, K. (2015) Mediterranean climate and oceanography, and the periodic development of anoxic events (sapropels). *Earth-Science Reviews* 143, 62–97.

Scott, C., Lyons, T.W. (2012) Contrasting molybdenum cycling and isotopic properties in euxinic versus non-euxinic sediments and sedimentary rocks: Refining the paleoproxies. *Chemical Geology* 324, 19–27.

Tossell, J. (2005) Calculating the partitioning of the isotopes of Mo between oxidic and sulfidic species in aqueous solution. *Geochimica et Cosmochimica Acta* 69, 2981–2993.

Ziegler, M., Tuenter, E., Lourens, L.J. (2010) The precession phase of the boreal summer monsoon as viewed from the eastern Mediterranean (ODP Site 968). *Quaternary Science Reviews* 29, 1481–1490.

Geochemical Perspectives Letters

Molybdenum isotope constraints on the temporal development of sulfidic conditions during Mediterranean sapropel intervals

T.C. Sweere, R. Hennekam, D. Vance, G-J. Reichart

Supplementary Information

The Supplementary Information includes:

- Material and Methods
- Results
- Comparison with Other Sapropel S5 Data
- Alternative Models for Low δ^{98}Mo Values
- Supplementary Information References

Material and Methods

The multi-core (MC, containing sapropel S1) and piston core (PC, containing sapropels S3 to S9) at location 64PE406-E1 (33°18.1'N, 33°23.7'E) was recovered from 1760 m water depth (Bale *et al.*, 2019). The core was scanned at mm-scale using an Avaatech XRF Core Scanner (XCS) at the NIOZ (see Hennekam *et al.*, 2019, 2020 for details) and Mo counts were converted to concentrations using ICP-MS analysis on discrete samples and a multivariate log-ratio approach for calibration (Weltje *et al.*, 2015; Bale *et al.*, 2019; Hennekam *et al.*, 2020). Bulk rock digests were spiked with a ^{100}Mo-^{97}Mo double spike (Klaver and Coath, 2019) and Mo was separated from matrix and interferences using a scaled-down down (~10-fold, 200 µl resin-bed) version of a column chromatography procedure with AG1-X8 resin (Dickson *et al.*, 2016). Mo-isotope data were measured in 2 % HNO_3 on a Thermo Scientific Neptune Plus MC-ICP-MS at the NIOZ and reported as $\delta^{98}Mo = [^{98/95}Mo_{sample}/^{98/95}Mo_{NIST} -$

1] x 1000 + 0.25. The external reproducibility was estimated by analysis of the SDO-1 rock standard (1.00 ± 0.06 ‰, 2 s.d., n = 11). The age model of core 64PE406-E1 was constructed by alignment of sapropel boundaries for sapropels S1 to S' with well-dated nearby cores, *i.e.* LC21 (Grant *et al.*, 2016) for sapropels S1 to S5 and ODP 968 (Ziegler *et al.*, 2010) for Sapropels S6 to S'.

Results

δ^{98}Mo values range from -0.67 to +2.13 ‰ with an average of 0.91 ‰ (n = 64, Fig. S-1). The data table is available for download (Excel file) at https://www.geochemicalperspectivesletters.org/article2108. All samples are highly enriched in Mo relative to upper continental crust compositions, with Mo_{EF} (= $[Mo/Al]_{sample}/[Mo/Al]_{detrital}$) ranging from 21 to 201 with an average of 97, for an $Mo/Al_{detrital}$ ratio of 11.9 x 10^{-6} (Taylor and McLennan, 1985; Andersen *et al.*, 2018). Lowest δ^{98}Mo values (-0.4 to +0.2 ‰) are registered for sapropels S3 and S9. Together with S4 and S8, these sapropels also generally show the lowest Mo concentrations (<62 ppm for samples measured by ICP-MS). Highest δ^{98}Mo values (<2.13 ‰) and Mo concentrations (<140 ppm) are found for sapropels S5 and S7. Sapropel S6 shows intermediate Mo concentrations (<103 ppm) and δ^{98}Mo values (<1.53 ‰).

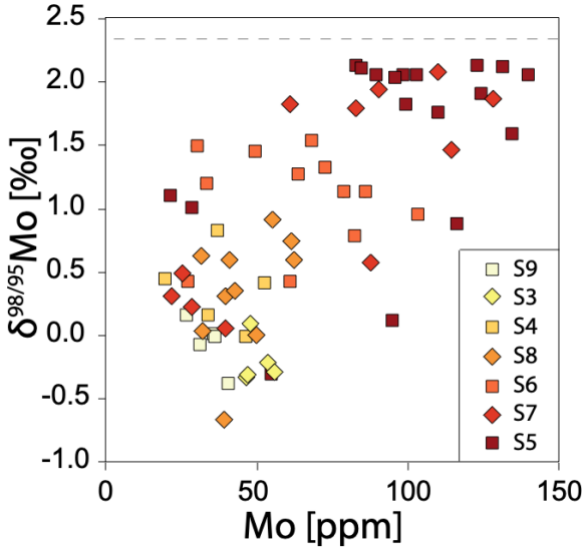

Figure S-1 δ^{98}Mo values relative to Mo concentrations for the different sapropels.

Comparison with other sapropel S5 data

Stratigraphic trends and absolute values of δ^{98}Mo and Mo concentrations of the sapropel S5 data presented in this study are generally very similar to previously published data (Fig. S-2; ODP 967 C, Andersen *et al.*, 2018). The main difference between the two datasets is found near the onset of the sapropel interval, where data from the 64PE406-E1 core (this study) show considerably lower δ^{98}Mo values. This difference might be the result of the depth difference between the two locations. Larger isotopic fractionation between sediments and seawater might have been preserved for the 64PE406-E1 core location due to less reducing conditions at shallower depths. Alternatively, the lower sample resolution of the ODP 967 C core data might exclude the short perturbation to lower δ^{98}Mo values.

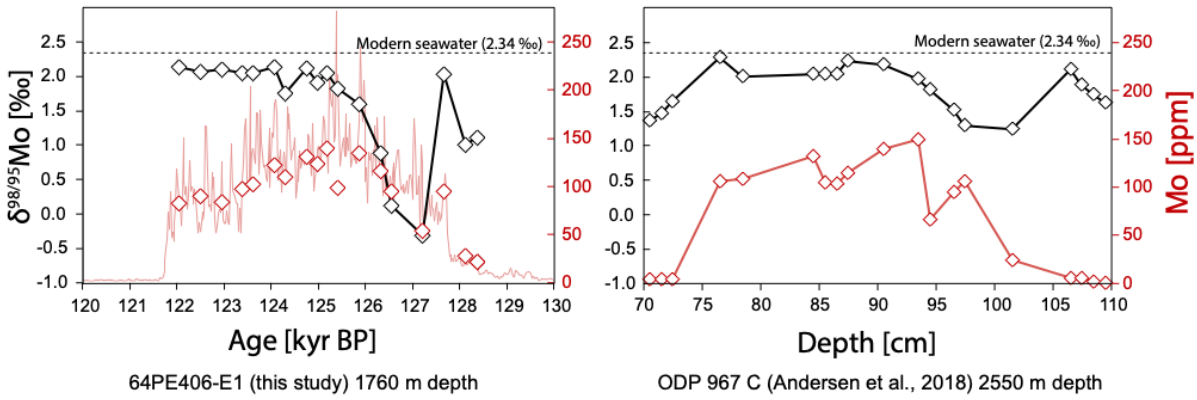

Figure S-2 Comparison of sapropel S5 Mo concentration and isotope data for the 64PE406-E1 core (this study) and ODP 967 C (Andersen *et al.*, 2018).

Alternative models for low δ^{98}Mo values

The main manuscript focuses on the interpretation of Mo-isotope patterns as a result of varying H_2S concentrations. It suggests that low δ^{98}Mo values are the result of deposition in mildly euxinic conditions, as has also been proposed for sediments from the sapropel S1 interval (Azrieli-Tal *et al.*, 2014; Matthews *et al.*, 2017; Andersen *et al.*, 2020). However, other models for low δ^{98}Mo values in

sapropel or organic-rich sediments have also been suggested. The relevance of these alternative theories for low δ^{98}Mo values of the sapropel S3 to S9 data presented here will be discussed below.

Oxic (MnO_x) deposition and diagenetic alteration. Reitz *et al*. (2007) proposed that low δ^{98}Mo values for the partly oxidised sapropel S1 are the result of original oxic deposition of isotopically light Mo (MnO_x adsorption) and subsequent diagenetic alteration. This interpretation is largely based on an extremely high peak in Mn concentrations (up to ~25 %) for the oxidised top of the sapropel, which is associated with the highest Mo concentrations. The authors hypothesise that deposition of MnO_x was associated with adsorbed isotopically light Mo that was subsequently released to sedimentary pore waters during reductive dissolution of MnO_x. A fraction of the released Mo might have diffused upwards and precipitate with MnO_x at shallower sediment depths, whereas secondary uptake of Mo by authigenic sulphides might have led to additional Mo-isotope fractionation deeper in the sediment, possibly resulting in even lower δ^{98}Mo values. Later studies from other locations have generally suggested that low δ^{98}Mo values for the sapropel S1 interval are the result of large isotope fractionation from seawater under mildly euxinic conditions (Azrieli-Tal *et al*., 2014; Matthews *et al*., 2017; Andersen *et al*., 2020).

Mn concentration data for sapropels S3 to S9 do not provide direct support for the alternative model of MnO_x deposition as an explanation for low δ^{98}Mo values for these sapropels (Figs. S-3 and S-4). While depth intervals of enhanced Mn enrichments are observed for some sapropels, these peaks occur below the sapropel intervals and concentrations are much lower (<2 %) than Mn concentrations found near the top of the oxidised S1 interval (Fig. S-4). Samples with high Mn concentrations are not associated with high Mo concentrations or low δ^{98}Mo values (Fig. S-3). Additionally, low δ^{98}Mo values are found even for sapropels without increases in Mn concentrations around the sapropel interval (*e.g.*, S8 and S9). We therefore do not find direct support for original oxic deposition (MnO_x adsorption) as an explanation for low δ^{98}Mo values for the studied sapropels.

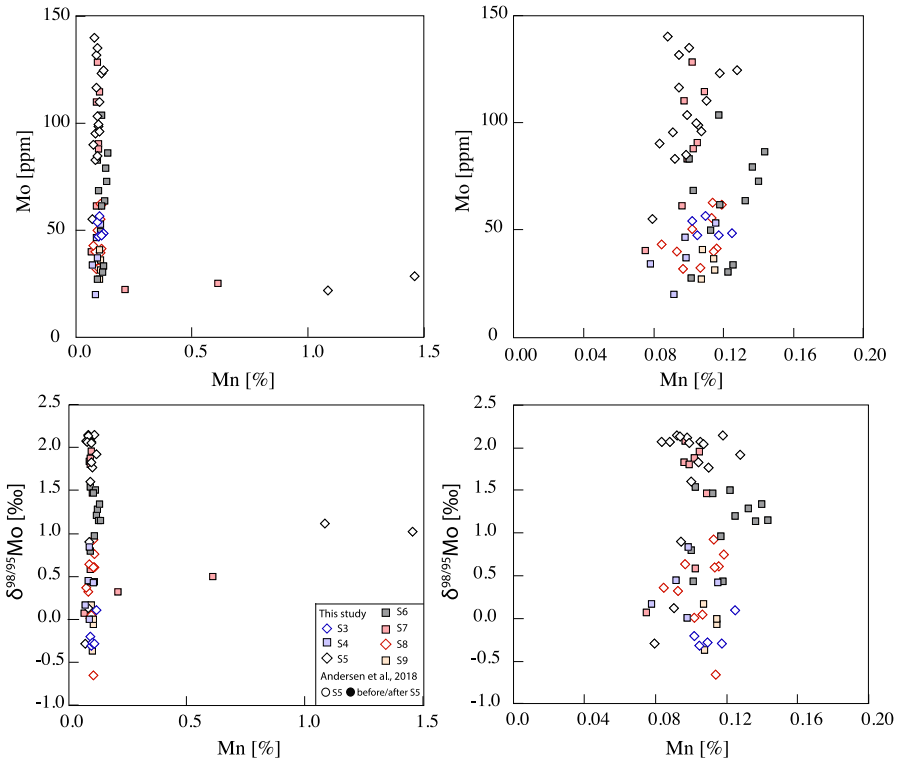

Figure S-3 δ^{98}Mo values and Mo concentrations relative to Mn concentrations. Apart from four outliers, Mn concentrations are generally low (<0.15 %). No correlations between Mn and Mo are observed.

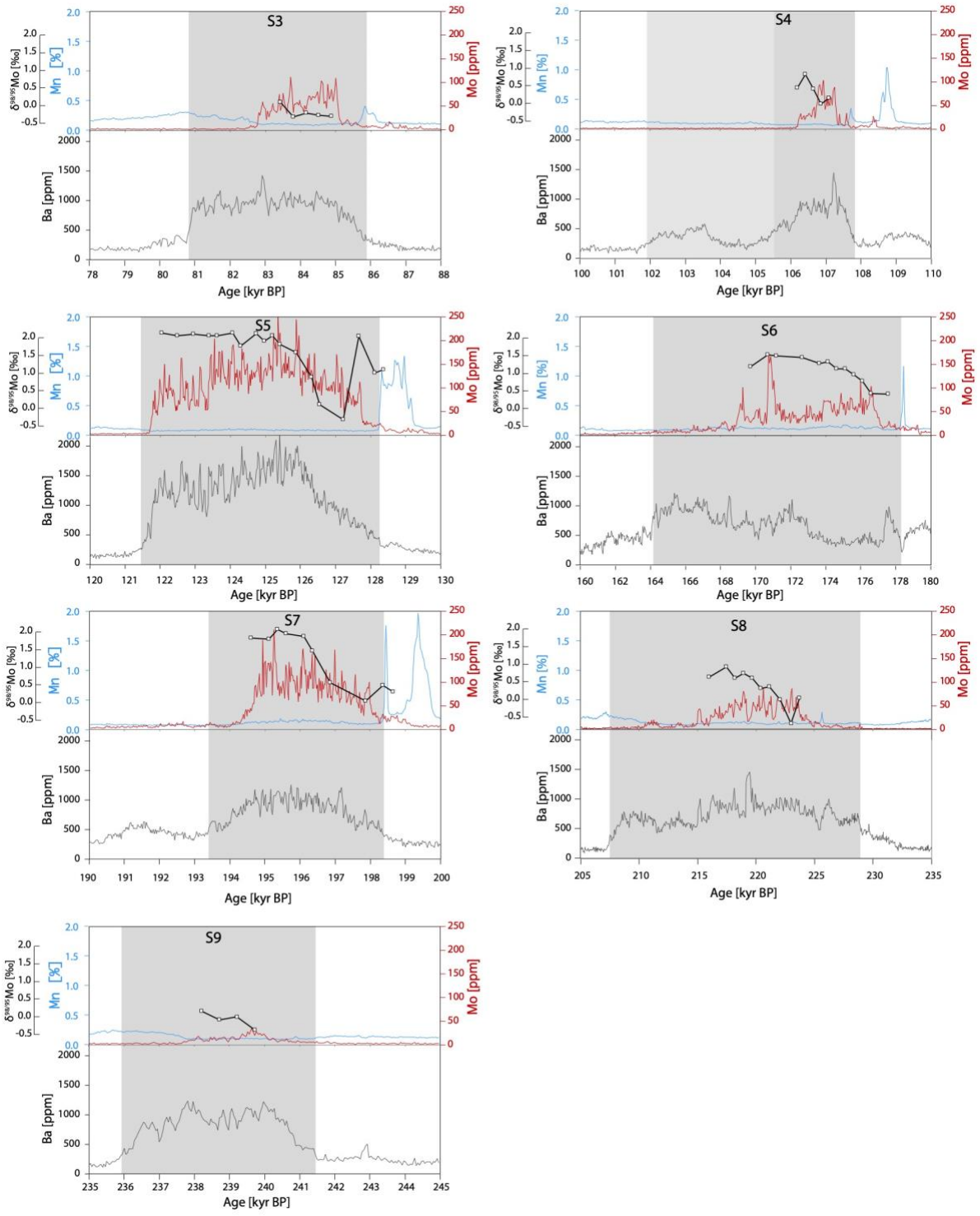

Figure S-4 Stratigraphic presentation Mo-isotope data with Ba, Mn, and Mo concentrations by XRF core scanning. The grey bands reflect the sapropel intervals as based on Ba enrichments.

Fe-Mn particulate shuttle. The delivery of isotopically light particulate Mo to the sediment with Fe (oxyhydr)oxides has also been suggested to cause light Mo-isotope signatures in some settings (*e.g.*, Scholz *et al.*, 2017). A so-called Fe-Mn particulate shuttle may result in the enhanced transport of isotopically light Mo to the sediment followed by capture in authigenic Mo-S phases during early diagenesis (Algeo and Tribovillard, 2009). This process is considered to be particularly important in settings with oxic surface waters and nitrogenous deep waters, especially where short time-scale changes in redox conditions occur, as this allows the efficient shuttle of particulate Mo to the sediment because reactive Fe can repeatedly be recycled. Mo_{EF} *vs* U_{EF} cross-plots can provide insight in whether this particulate shuttle was a relevant mechanism for Mo enrichment during sapropel deposition as this process will not affect U enrichments (Algeo and Tribovillard, 2009). High Mo enrichments relative to U may therefore point to an active particulate Mo shuttle (Algeo and Tribovillard, 2009).

Mo_{EF} and U_{EF} patterns for the studied sapropels generally follow the unrestricted open marine trend and approach seawater values during peak-sapropel intervals, in agreement with previously published S1 and S5 data (Azrieli-Tal *et al.*, 2014; Matthews *et al.*, 2017; Andersen *et al.*, 2018). These observations do not suggest that enhanced enrichment of Mo due to a strong Fe-Mn particulate shuttle was relevant during sapropel deposition. We therefore do not find direct support for an Fe-Mn particulate shuttle as an explanation for the low δ^{98}Mo values for these sapropels and conclude that these likely derive from a large isotopic fractionation in mildly euxinic conditions, as also suggested in recent studies of sapropel S1 (Azrieli-Tall *et al.*, 2014; Matthews *et al.*, 2017; Andersen *et al.*, 2020).

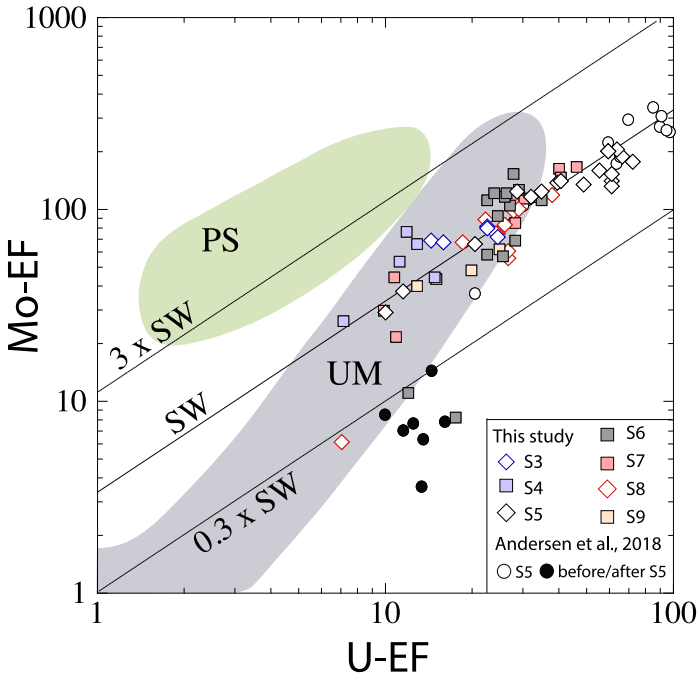

Figure S-5 Mo_{EF} *versus* U_{EF} cross-plots after Algeo and Tribovillard (2009). The green area reflects enhanced Mo enrichment linked to operation of an Fe-Mn particulate shuttle, whereas the grey area reflects values found in unrestricted marine conditions. Samples from sapropel intervals generally plot close to the open ocean seawater ratio. Previously published S5 data is added for comparison (Andersen *et al.*, 2018).

Supplementary Information References

Algeo, T.J., Tribovillard, N. (2009) Environmental analysis of paleoceanographic systems based on molybdenum–uranium covariation. *Chemical Geology* 268, 211-225.

Andersen, M.B., Matthews, A., Vance, D., Bar-Matthews, M., Archer, C., de Souza, G. (2018) A 10-fold decline in the deep Eastern Mediterranean thermohaline overturning circulation during the last interglacial period. *Earth and Planetary Science Letters* 503, 58-67.

Andersen, M.B., Matthews, A., Bar-Matthews, M. Vance, D. (2020) Rapid onset of ocean anoxia shown by high U and low Mo isotope compositions of sapropel S1. *Geochemical Perspectives Letters* 15, 10-14.

Azrieli-Tal, I., Matthews, A., Bar-Matthews, M., Almogi-Labin, A., Vance, D., Archer, C., Teutsch, N. (2014) Evidence from molybdenum and iron isotopes and molybdenum–uranium covariation for sulphidic bottom waters during Eastern Mediterranean sapropel S1 formation. *Earth and Planetary Science Letters* 393, 231-242.

Bale, N.J., Hennekam, R., Hopmans, E.C., Dorhout, D., Reichart, G.-J., van der Meer, M., Villareal, T.A., Sinninghe Damsté, J.S., Schouten, S. (2019) Biomarker evidence for nitrogen-fixing cyanobacterial blooms in a brackish surface layer in the Nile River plume during sapropel deposition. *Geology* 47, 1088-1092.

Dickson, A.J., Jenkyns, H.C., Porcelli, D., van den Boorn, S., Idiz, E. (2016) Basin-scale controls on the molybdenum-isotope composition of seawater during Oceanic Anoxic Event 2 (Late Cretaceous). *Geochimica et Cosmochimica Acta* 178, 291-306.

Grant, K., Grimm, R., Mikolajewicz, U., Marino, G., Ziegler, M., Rohling, E. (2016) The timing of Mediterranean sapropel deposition relative to insolation, sea-level and African monsoon changes. *Quaternary Science Reviews* 140, 125-141.

Hennekam, R., Sweere, T., Tjallingii, R., de Lange, G.J., Reichart, G.-J. (2019) Trace metal analysis of sediment cores using a novel X-ray fluorescence core scanning method. *Quaternary International* 514, 55-67.

Hennekam, R., van der Bolt, B., van Nes, E.H., de Lange, G.J., Scheffer, M., Reichart, G.-J. (2020) Early-warning signals for marine anoxic events. *Geophysical Research Letters* 47, e2020GL089183.

Klaver, M., Coath, C.D. (2019) Obtaining Accurate Isotopic Compositions with the Double Spike Technique: Practical Considerations. *Geostandards and Geoanalytical Research* 43, 5-22.

Matthews, A., Azrieli-Tal, I., Benkovitz, A., Bar-Matthews, M., Vance, D., Poulton, S.W., Teutsch, N., Almogi-Labin, A., Archer, C. (2017) Anoxic development of sapropel S1 in the Nile Fan inferred from redox sensitive proxies, Fe speciation, Fe and Mo isotopes. *Chemical Geology* 475, 24-39.

Reitz, A., Wille, M., Nägler, T.F., de Lange, G.J. (2007) Atypical Mo isotope signatures in eastern Mediterranean sediments. *Chemical Geology* 245, 1-8.

Rudnick, R.L., Gao, S. (2003) Composition of the continental crust. In: Holland, H., Turekian, K. (Eds.) *Treatise on Geochemistry*, Second Edition. Elsevier, 1-64.

Scholz, F., Siebert, C., Dale, A.W., Frank, M. (2017) Intense molybdenum accumulation in sediments underneath a nitrogenous water column and implications for the reconstruction of paleo-redox conditions based on molybdenum isotopes. *Geochimica et Cosmochimica Acta* 213, 400-417.

Taylor R.N., McLennan, S. (1985) *The Continental Crust: Its Composition and Evolution*. Blackwell, Boston.

Weltje, G.J., Bloemsma, M., Tjallingii, R., Heslop, D., Röhl, U., Croudace, I.W. (2015) Prediction of geochemical composition from XRF core scanner data: a new multivariate approach including

automatic selection of calibration samples and quantification of uncertainties. In: Croudace, I.W., Rothwell, R.G. (Eds.) *Micro-XRF Studies of Sediment Cores*. Springer, Dordrecht, 507-534.

Ziegler, M., Tuenter, E., Lourens, L.J. (2010) The precession phase of the boreal summer monsoon as viewed from the eastern Mediterranean (ODP Site 968). *Quaternary Science Reviews* 29, 1481-1490.